

Sensitivity of symmetry energy elements of nuclear matter to the properties of neutron rich systems

C. Mondal, B. K. Agrawal,* J. N. De, and S. K. Samaddar

Saha Institute of Nuclear Physics, 1/AF Bidhannagar, Kolkata 700064, India

The sensitivity of nuclear symmetry energy elements at the saturation density to the binding energies of ultra neutron-rich nuclei (neutron to proton ratio ~ 2) and the maximum mass of neutron star is explored within a relativistic mean field model. Values of the interaction parameters governing the isovector strengths and the symmetry elements are determined in tighter bounds. Assessments based on the sensitivity matrix reveal that the properties of extreme neutron-rich systems play a predominant role in narrowing down the uncertainties in the various symmetry energy parameters. The calculations are extended over a wide range of nuclear matter density and the results are discussed.

PACS numbers: 21.30.Fe, 21.65.Ef, 21.60.Jz

I. INTRODUCTION

The binding energies of atomic nuclei are the most accurately determined data in nuclear physics. All informations about nuclear interactions are firmly entrenched in them. Ideas have been proposed in recent years to establish precision values of isovector indicators in nuclear interactions (like the volume and surface symmetry energy coefficients C_v^0 and C_s of nuclei, the density slope parameter L_0 of symmetry energy or the neutron skin Δr_{np} of heavy nuclei) from nuclear masses. Using the nuclear droplet model designed to explain nuclear masses, from correlation systematics of Δr_{np} of ^{208}Pb with nuclear isospin, Centelles *et al* [1] get $L_0 = 75 \pm 25$ MeV. Fitting few thousand observed nuclear masses within the finite range droplet model (FRDM) [2] Möller *et al* find C_v^0 to be 32.5 ± 0.5 MeV, L_0 comes out to be 70 ± 15 MeV. From double differences of symmetry energies estimated from the nuclear masses, Jiang *et al* [3] get $C_v^0 = 32.10 \pm 0.31$ MeV and the surface symmetry energy coefficient C_s is determined to be 58.91 ± 1.08 MeV. These informations coupled with microscopic calculations on nucleon distributions [4–6] in a heavy nucleus like ^{208}Pb give $L_0 = 59 \pm 13$ MeV and the neutron skin Δr_{np} of ^{208}Pb to be $\sim 0.195 \pm 0.021$ fm. With progression in time, analyses based on nuclear masses seem to contain the fluctuations in the symmetry observables better [2, 3, 7–9], better compared to those obtained from isoscaling [10], nuclear emission ratios [11], isospin diffusion [12], giant dipole polarizability [13], quadrupole resonances [14] or from astrophysical evidences [15].

Microscopic mean-field models, both non-relativistic and relativistic with energy density functionals (EDF) parametrized to give best fits to nuclear masses and also to some other selective isoscalar and isovector-sensitive observables, however, do not show such constraints in

the values of C_v^0 or L_0 [16–20]. They have much wider variations. This looks like a puzzle. As an example, the isovector sensitive binding energy difference ΔB of ^{132}Sn and ^{100}Sn shows nearly no correlation between ΔB and Δr_{np} for ^{132}Sn for different set of Skyrme interactions [21]. The binding energy difference in different EDFs are reproduced fairly well, but Δr_{np} shows a wide variation.

In a recent calculation [22] in the relativistic mean field model (RMF), attempts were made to understand this seeming paradox. The binding energy difference between four pairs of nuclei, namely (^{68}Ni - ^{56}Ni), (^{132}Sn - ^{100}Sn), (^{24}O - ^{16}O) and (^{30}Ne - ^{18}Ne) calculated in 14 different RMF models when plotted against the computed values of Δr_{np} of ^{208}Pb in the same models shows increasingly high correlation with increasing asymmetry. The asymmetry δ is defined as $\delta = (N - Z)/A$ where N and Z are the neutron and proton numbers in a nucleus of mass number A . This is suggestive of the fact that isovector part of the nuclear interaction would be better constrained if nuclei of higher asymmetries are included in the binding energy systematics. A covariance analysis displaying correlation among physical observables makes this fact more revealing. That the choice of very neutron-rich isotopes is more rewarding for the searching of isovector signatures was also found recently by Chen and Piekarewicz [23].

The present communication is a follow-up of our earlier paper [22] and to see if the conclusions so drawn in Refs. [22, 23] stand a broader systematic analysis. The sensitivity of symmetry energy elements of nuclear matter at saturation density to different properties of highly neutron rich systems are analyzed here in detail. For this, we have chosen an expanded data set of nuclear masses with inclusion of nuclei of very high isospin ($\delta > 0.3$). Since neutron star is composed mainly of nuclear matter of extreme isospin, we have also included the observed maximum mass of neutron star as an element in the fitting protocol. The analysis is also extended over a wide range of nuclear matter density.

The paper is organized as follows. The effective Lagrangian density for the RMF model employed in the

*Electronic address: bijay.agrawal@saha.ac.in

TABLE I: Optimum values of the parameters for the models SINPB and SINPA, uncorrelated (upper line) and correlated (lower line) errors on them are given in the parentheses. Mass of the σ meson (m_σ) is given in units of MeV. The masses of ω and ρ mesons are kept fixed to $m_\omega = 782.5$ MeV and $m_\rho = 763$ MeV and nucleon mass is taken to be $M = 939$ MeV.

Name	g_σ	g_ω	g_ρ	κ_3	κ_4	$\eta_{2\rho}$	ζ_0	m_σ
SINPB	-10.6007	13.8767	10.613	1.4868	-0.802	13.487	5.467	493.850
	(0.0001)	(0.0002)	(0.036)	(0.0002)	(0.002)	(0.312)	(0.003)	(0.006)
	(0.14)	(0.24)	(1.29)	(0.19)	(1.15)	(12.26)	(0.45)	(4.98)
SINPA	-10.6292	13.8532	12.831	1.5375	-1.190	38.179	5.363	495.394
	(0.0001)	(0.0002)	(0.043)	(0.0002)	(0.002)	(0.521)	(0.003)	(0.006)
	(0.16)	(0.33)	(0.82)	(0.06)	(0.47)	(11.92)	(0.45)	(3.86)

present work is briefly outlined in Sec. II. The results obtained by optimizing the objective function for different sets of fit-data and the analysis pertaining to the sensitivity of various symmetry energy parameters to the properties of neutron rich systems are discussed in Sec. III. The summary and conclusions are given in Sec. IV.

II. EFFECTIVE LAGRANGIAN

The effective Lagrangian density for the RMF model used in this present work is similar to that of FSU [24–27]. Its interaction part is given by,

$$\begin{aligned} \mathcal{L}_{int} = & \bar{\psi} \left[g_\sigma \sigma - \gamma^\mu \left(g_\omega \omega_\mu + \frac{1}{2} g_\rho \boldsymbol{\tau} \cdot \boldsymbol{\rho}_\mu + \frac{e}{2} (1 + \tau_3) A_\mu \right) \right] \psi \\ & - \frac{\kappa_3}{6M} g_\sigma m_\sigma^2 \sigma^3 - \frac{\kappa_4}{24M^2} g_\sigma^2 m_\sigma^2 \sigma^4 + \frac{1}{24} \zeta_0 g_\omega^2 (\omega_\mu \omega^\mu)^2 \\ & + \frac{\eta_{2\rho}}{4M^2} g_\omega^2 m_\rho^2 \omega_\mu \omega^\mu \boldsymbol{\rho}_\nu \boldsymbol{\rho}^\nu. \end{aligned} \quad (1)$$

It comprises the conventional Yukawa couplings between the nucleonic field ψ and the mesonic fields σ , ω and ρ with coupling constants g_σ , g_ω and g_ρ , respectively. The parameter g_σ stands for the long-range attractive nature of the nuclear force. Its repulsive nature at short ranges is taken care of by the parameter g_ω . The cubic and quartic self couplings of σ meson are characterized by the parameters κ_3 and κ_4 , respectively. The parameter ζ_0 symbolizes the strength of the quartic self coupling of ω meson. All these self-couplings render an added softening in the equation of state (EoS) of symmetric nuclear matter. The density dependence of symmetry energy of nuclear matter is governed by the coupling constants g_ρ and $\eta_{2\rho}$; $\eta_{2\rho}$ represents the strength of the cross-coupling between ω and ρ mesons. The parameter $\eta_{2\rho}$ provides some added flexibility in fitting the ground state properties of some standard doubly magic spherical nuclei and yet allowing the value of the neutron skin Δr_{np} of ^{208}Pb to vary over a wide range [28, 29]. The strength of the electromagnetic interaction between the protons is described by the coupling constant e .

III. RESULTS AND DISCUSSIONS

To analyze the sensitivity of the symmetry energy elements of nuclear matter to highly neutron rich systems, two different RMF models are constructed, one with inclusion of few ultra neutron-rich systems in the fitted data and another without them. A comparative study on the nuclear matter properties of these two models is executed in detail. We performed a comprehensive study to find the isovector signatures from those highly neutron rich systems from different perspectives. At the end, different properties of nuclear matter beyond saturation are critically examined.

A. The RMF models SINPB and SINPA

The values of the parameters (\mathbf{p}) which describe the EDF of the RMF model (Eq. (1)) are obtained by optimizing the objective function $\chi^2(\mathbf{p})$ defined as,

$$\chi^2(\mathbf{p}) = \frac{1}{N_d - N_p} \sum_{i=1}^{N_d} \left(\frac{\mathcal{O}_i^{exp} - \mathcal{O}_i^{th}(\mathbf{p})}{\Delta \mathcal{O}_i} \right)^2. \quad (2)$$

Here, $(N_d - N_p)$ is the degrees of the freedom of the system given by the difference between the number of experimental data points N_d and number of fitted parameters N_p . The experimental and the corresponding theoretically obtained value of an observable are given by \mathcal{O}_i^{exp} and $\mathcal{O}_i^{th}(\mathbf{p})$, respectively. $\Delta \mathcal{O}_i$ is the adopted error of an observable. The minimum value of the objective function χ_0^2 corresponds to the value of χ^2 at \mathbf{p}_0 , \mathbf{p}_0 being the optimal values of the parameters.

After optimization [30], variance on a quantity \mathcal{A} , $\overline{\Delta \mathcal{A}^2}$ can be evaluated as,

$$\overline{\Delta \mathcal{A}^2} = \sum_{\alpha\beta} \left(\frac{\partial \mathcal{A}}{\partial p_\alpha} \right)_{\mathbf{p}_0} C_{\alpha\beta}^{-1} \left(\frac{\partial \mathcal{A}}{\partial p_\beta} \right)_{\mathbf{p}_0}, \quad (3)$$

where \mathcal{A} could be parameters as well as observables. Here $C_{\alpha\beta}^{-1}$ is an element of inverted curvature matrix given by,

$$C_{\alpha\beta} = \frac{1}{2} \left(\frac{\partial^2 \chi^2(\mathbf{p})}{\partial p_\alpha \partial p_\beta} \right)_{\mathbf{p}_0}. \quad (4)$$

From Eq. (3) one can see that, the diagonal element $\mathcal{C}_{\alpha\alpha}^{-1}$ of the inverted curvature matrix is the variance on the parameter p_α .

TABLE II: Various observables \mathcal{O} , adopted errors on them $\Delta\mathcal{O}$, corresponding experimental data (Expt.) and their best-fit values for SINPB and SINPA. B and r_{ch} corresponds to binding energy and charge radius of a nucleus, respectively and M_{max}^{NS} is the maximum mass of neutron star (NS). Values of B are given in units of MeV and r_{ch} in fm. M_{max}^{NS} is in units of Solar Mass (M_\odot).

	\mathcal{O}	$\Delta\mathcal{O}$	Expt.	SINPB	SINPA
^{16}O	B	4.0	127.62	127.78	128.35
	r_{ch}	0.04	2.699	2.704	2.696
^{24}O	B	2.0	168.96	-	169.28
^{20}Ne	B	4.0	160.64	-	155.89
^{30}Ne	B	3.0	211.29	-	214.37
^{24}Mg	B	3.0	198.26	-	195.87
^{36}Mg	B	2.0	260.78	-	261.68
^{40}Ca	B	3.0	342.05	343.19	343.66
	r_{ch}	0.02	3.478	3.460	3.452
^{48}Ca	B	1.0	416.00	415.27	415.47
	r_{ch}	0.04	3.477	3.437	3.437
^{54}Ca	B	2.0	445.37	445.63	443.79
^{58}Ca	B	2.0	454.43	-	456.33
^{56}Ni	B	5.0	483.99	483.38	484.34
	r_{ch}	0.18	3.750	3.700	3.686
^{68}Ni	B	2.0	590.41	592.86	592.97
^{78}Ni	B	2.0	641.78	642.10	641.59
^{90}Zr	B	1.0	783.90	783.02	783.20
	r_{ch}	0.02	4.269	4.266	4.264
^{100}Sn	B	2.0	825.30	828.11	827.93
^{116}Sn	B	2.0	988.68	987.45	987.32
	r_{ch}	0.18	4.625	4.620	4.622
^{132}Sn	B	1.0	1102.84	1103.28	1103.40
	r_{ch}	0.02	4.709	4.706	4.710
^{138}Sn	B	2.0	1119.59	1118.65	1117.05
^{144}Sm	B	2.0	1195.73	1196.00	1195.67
	r_{ch}	0.02	4.952	4.955	4.955
^{208}Pb	B	1.0	1636.43	1636.38	1636.57
	r_{ch}	0.02	5.501	5.528	5.530
NS	M_{max}^{NS}	0.04	2.01	-	1.98

To explore the information content of some of the highly neutron rich systems, two models, namely, SINPB and SINPA are constructed. In SINPB binding energies (B) and charge radii (r_{ch}) of some standard set of nuclei across the whole nuclear chart are taken as fit-data (see Tab. II). The binding energies of ^{54}Ca , ^{78}Ni and ^{138}Sn nuclei having somewhat larger asymmetry ($\delta \sim 0.26 - 0.28$) are also included in the fitting protocol. The model SINPA includes some highly asymmetric nuclei, namely, ^{24}O , ^{30}Ne , ^{36}Mg and ^{58}Ca ($\delta > 0.3$) in addition

to the data set used in the base model SINPB. SINPA also contains the symmetric ^{20}Ne and ^{24}Mg nuclei and the observed maximum mass of neutron star M_{max}^{NS} as fit-data.

In Table I, the optimal values of the parameters \mathbf{p}_0 for SINPB and SINPA are given along with the uncorrelated and correlated errors on them. Correlated or uncorrelated errors can be calculated from Eq. (3) by including or excluding the contribution from the off-diagonal elements of curvature matrix $\mathcal{C}_{\alpha\beta}$, respectively. One can observe that the correlated errors (lower lines inside the parentheses in Table I) on the parameters g_ρ , κ_3 , κ_4 and m_σ decreased by a noticeable amount in SINPA in comparison to SINPB. For the parameters g_σ , ζ_0 and $\eta_{2\rho}$ the errors are almost the same for both the models and for the case of g_ω its value is slightly higher in SINPA than in SINPB. The pairing is treated within the BCS approximation with cut-off energy in pairing space taken as $\hbar\omega_0 = 41A^{-1/3}$ MeV. The BCS pairing strengths for neutron and proton for the models SINPB and SINPA were kept fixed to $G_n = 20/A$ and $G_p = 25/A$. The neutron and proton pairing gaps (Δ_n, Δ_p) in MeV for the neutron rich nuclei are ^{30}Ne (0.0, 2.3), ^{36}Mg (2.5, 2.0), ^{54}Ca (1.1, 0.0), ^{58}Ca (1.0, 0.0), ^{138}Sn (1.3, 0.0). The pairing gaps for other non-magic nuclei are close to $12/\sqrt{A}$ MeV. The neutron pairing gap for ^{24}O practically vanishes, since, the first unoccupied $1d_{3/2}$ orbit is about 4.5 MeV above the completely filled $2s_{1/2}$ orbit [23].

In Table II different observables \mathcal{O} pertaining to finite nuclei and neutron star, their experimental values, their obtained values from SINPB and SINPA along with $\Delta\mathcal{O}$, the adopted errors on them are listed. The experimental values of binding energies of all the nuclei except for ^{54}Ca used in the fit are taken from the latest compilation AME-2012 [31]. Recently, binding energy of ^{54}Ca was measured very accurately at TRIUMF [32] and CERN [33]. For this present calculation, the experimental value of the binding energy for ^{54}Ca is taken from Ref. [33]. Experimental values for the charge radii used in the fit are obtained from the compilation by Angeli and Marinova [34]. For the optimization of SINPA, observed maximum mass of neutron star M_{max}^{NS} is taken from Ref. [35, 36]. It may be pointed out that, experimental value for some of the fit data are little different in the present calculation in comparison to our previous paper [22]. Except for ^{68}Ni , $\Delta\mathcal{O}$ for all the fit-data common to both the models SINPB and SINPA are taken from Ref. [37]. As the obtained value of binding energy of ^{68}Ni from both the models SINPB and SINPA deviate by more than 2 MeV from its experimental value, demanding too much accuracy on that particular datum costs a larger amount in total χ^2 compared to other data points. For this reason we have taken $\Delta\mathcal{O} = 2$ MeV for the binding energy of ^{68}Ni unlike in Ref.[37], where $\Delta\mathcal{O} = 1$ MeV. Calculated errors on the binding energies and charge radii due to uncertainties in the model parameters for the fitted nuclei for both the models SINPB and SINPA lie within the range from 0.51 - 1.89 MeV and 0.005 - 0.016 fm, respec-

tively. In model SINPA the obtained maximum neutron star mass M_{max}^{NS} ($1.98 \pm 0.03 M_\odot$) compares well with the observed value. We would like to point out that the two isotopes of Mg nuclei used in the optimization of SINPA are deformed. The numerical computation is done with 20 oscillator shells being taken as the basis states for the nucleons. The quadrupole deformation parameter β_2 calculated from SINPA for ^{24}Mg and ^{36}Mg nuclei are found to be 0.47 and 0.37, respectively.

B. Nuclear Matter Properties

The energy per nucleon in asymmetric nuclear matter as a function of density ρ and isospin asymmetry δ is approximately given by,

$$\mathcal{E}(\rho, \delta) = \mathcal{E}(\rho, 0) + C_{sym}(\rho)\delta^2, \quad (5)$$

where, $\rho = (\rho_n + \rho_p)$ and $\delta = \frac{\rho_n - \rho_p}{\rho}$. The term $\mathcal{E}(\rho, 0)$ represents the energy per nucleon in symmetric nuclear matter and $C_{sym}(\rho)$ is the symmetry energy. Energy per nucleon $\mathcal{E}(\rho, 0)$ can be expressed in terms of model parameters as,

$$\begin{aligned} \mathcal{E}(\rho, 0) = & \frac{2}{\pi^2} \int_0^{k_F} dk k^2 \sqrt{k^2 + M^{*2}} \\ & + \frac{1}{2} m_\sigma^2 \sigma^2 + \frac{\kappa_3}{6M} g_\sigma m_\sigma^2 \sigma^3 + \frac{\kappa_4}{24M^2} g_\sigma^2 m_\sigma^2 \sigma^4 \\ & - \frac{1}{2} m_\omega^2 \omega^2 - \frac{1}{24} \zeta_0 g_\omega^2 \omega^4, \end{aligned} \quad (6)$$

and, $C_{sym}(\rho)$ is expressed as,

$$C_{sym}(\rho) = \frac{k_F^2}{6(k_F^2 + M^{*2})^{1/2}} + \frac{g_\rho^2}{12\pi^2} \frac{k_F^3}{m_\rho^{*2}}. \quad (7)$$

Here, k_F is the nucleon Fermi momentum in symmetric nuclear matter at density ρ ($= \frac{2k_F^3}{3\pi^2}$). The Dirac effective mass of nucleon M^* is given by,

$$M^* = M - g_\sigma \sigma, \quad (8)$$

and, the effective mass of ρ meson, m_ρ^* is expressed as [38],

$$m_\rho^{*2} = m_\rho^2 \left(1 + \frac{1}{2M^2} \eta_{2\rho} g_\omega^2 \omega^2 \right). \quad (9)$$

In the Eqs. (6-9) the value of the fields σ and ω are obtained by solving their field equation at a particular density ρ . From Eq. (7) one can see that, the kinetic part of $C_{sym}(\rho)$ depends on the effective mass of nucleon M^* , which has dependence on the parameter g_σ and the field value of σ . However, the interaction part of $C_{sym}(\rho)$ mainly depends on the isovector parameters g_ρ and $\eta_{2\rho}$. The value of the incompressibility coefficient K_0 at the saturation density is related to $\mathcal{E}(\rho, 0)$ as,

$$K_0 = 9 \left[\rho^2 \left(\frac{d^2 \mathcal{E}(\rho, 0)}{d\rho^2} \right) \right]_{\rho=\rho_0}. \quad (10)$$

TABLE III: Different nuclear matter properties: the binding energy per nucleon for symmetric matter \mathcal{E}_0 , incompressibility coefficient K_0 , Dirac effective mass of nucleon M_0^* (scaled by nucleon mass M), symmetry energy coefficient C_{sym}^0 and density slope parameter of symmetry energy L_0 for the nuclear matter evaluated at saturation density ρ_0 along with the correlated errors on them for the models SINPB and SINPA. The values of $C_{sym}(\rho_c)$ and $L(\rho_c)$ calculated at crossing density ρ_c along with the neutron skin Δr_{np} in ^{208}Pb are also presented for these two models.

Observable	SINPB	SINPA
\mathcal{E}_0 (MeV)	-16.04 ± 0.06	-16.00 ± 0.05
K_0 (MeV)	206 ± 20	203 ± 6
ρ_0 (fm^{-3})	0.150 ± 0.002	0.151 ± 0.001
M_0^*/M	0.59 ± 0.01	0.58 ± 0.01
C_{sym}^0 (MeV)	33.95 ± 2.41	31.20 ± 1.11
$C_{sym}(\rho_c)$ (MeV)	26.08 ± 0.41	25.60 ± 0.51
L_0 (MeV)	71.55 ± 18.89	53.86 ± 4.66
$L(\rho_c)$ (MeV)	55.98 ± 13.78	38.47 ± 5.43
Δr_{np} (^{208}Pb) (fm)	0.241 ± 0.040	0.183 ± 0.022

The symmetry energy slope parameter L at a given density ρ can be evaluated as,

$$L = 3\rho \left(\frac{dC_{sym}(\rho)}{d\rho} \right). \quad (11)$$

Once the objective functions for the models SINPB and SINPA are optimized, different nuclear matter properties can be extracted from them and compared. In Table III values of different nuclear matter parameters along with the corresponding errors evaluated within the covariance analysis are listed for SINPB and SINPA. The properties associated with symmetric nuclear matter are evaluated at the saturation density ρ_0 , while, those characterizing the asymmetric nuclear matter are evaluated at ρ_0 and the crossing-density ρ_c which is taken as $\frac{0.11}{0.16} \times \rho_0$ [39]. Errors on binding energy per nucleon \mathcal{E}_0 ($= \mathcal{E}(\rho_0, 0)$), saturation density ρ_0 and Dirac effective mass of nucleon M_0^*/M ($= M^*(\rho_0)/M$) are pretty much the same for both the models concerned. However, a noticeable improvement is observed for the model SINPA over SINPB for the calculated errors on the symmetry energy parameters C_{sym}^0 ($= C_{sym}(\rho_0)$), L_0 ($= L(\rho_0)$) and $L(\rho_c)$. The refinement in the error in SINPA in comparison to SINPB is also to be noted for the incompressibility coefficient at saturation density, K_0 . Error on the neutron-skin Δr_{np} in ^{208}Pb also reduces by almost a factor of 2 in SINPA in comparison to SINPB. The central values of L_0 and Δr_{np} of ^{208}Pb obtained for the model SINPB are seen to differ from those obtained from the model-I of Ref. [22]; this can be attributed to the differences in the adopted error on the binding energy of ^{68}Ni and to the differences in some of the experimental fit data.

The observation of improved constraint in the symmetry elements calculated from model SINPA over those

from SINPB clearly indicates that the additional data of four highly asymmetric nuclei (^{24}O , ^{30}Ne , ^{36}Mg and ^{58}Ca) with $\delta > 0.3$ and the observed maximum mass of neutron star M_{max}^{NS} contain more distilled information on isovector elements in the nuclear interaction. It is striking to note that the addition of the binding energies of ^{54}Ca , ^{78}Ni and ^{138}Sn ($\delta \sim 0.26-0.28$) as fit data in the optimization of the model SINPB did not improve the uncertainties in the symmetry energy parameters as compared to those for the model-I in Ref. [22]. On the other hand, inclusion of highly asymmetric ($\delta > 0.3$) ^{36}Mg and ^{58}Ca nuclei in the fitting protocol of the model SINPA yields smaller uncertainties in the symmetry energy parameters in comparison to the model-II of Ref. [22] which does not include these nuclei. This clearly emphasizes that the binding energies of nuclei with $\delta > 0.3$ play a crucial role in constraining the symmetry energy parameters and is thus a pointer to the necessity of taking data for very asymmetric nuclei in the optimization of the RMF model. In the next section we are going to analyze this more critically.

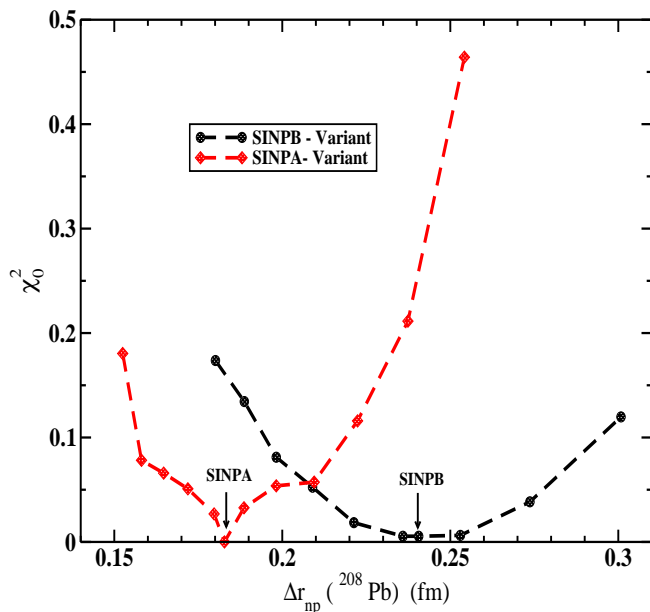


FIG. 1: (Color online) Optimum values of the objective function (χ_0^2) are plotted as a function of Δr_{np} (neutron skin of ^{208}Pb) for two families of models, namely, SINPB-Variant and SINPA-Variant (see text for details).

C. Sensitivity analysis

We now look into the sensitivity of symmetry energy parameters to the properties of the neutron rich systems in some detail. Before embarking on our analysis in terms of sensitivity matrix, we make a simple examination of the results. We look into the dependence of the optimal value of the objective function on the neutron skin of

^{208}Pb . Fixing $\eta_{2\rho}$ to a preset value and optimizing the χ^2 function by adjusting the rest of the model parameters, one can get a particular value of Δr_{np} of ^{208}Pb for the models SINPB and SINPA [29]. Two families of RMF models so constructed are called SINPB-Variant and SINPA-Variant. Different input values of $\eta_{2\rho}$ would yield different Δr_{np} in both these models. In Fig. 1 optimal values of the objective function χ^2 (i.e. χ_0^2) for these two models are displayed as a function of Δr_{np} of ^{208}Pb ; the values of χ_0^2 are so adjusted that their minimum value within a family vanishes. Visual comparison of results from the two families of models shows that there is a stronger preference to a particular value of Δr_{np} of ^{208}Pb

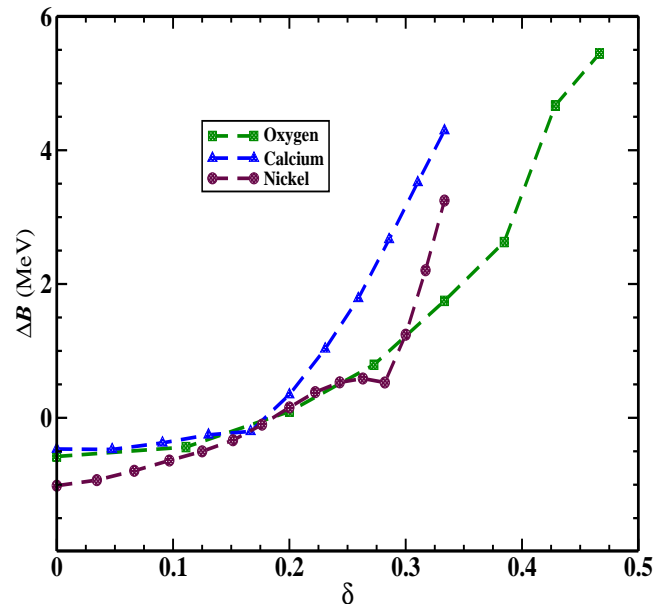


FIG. 2: (Color online) Binding energy differences ΔB ($=B(\text{SINPB}) - B(\text{SINPA})$) extracted using models SINPB and SINPA for even isotopes of O, Ca and Ni nuclei plotted as a function of asymmetry δ .

in the SINPA-Variant family. It is worthwhile to mention that, SINPB-Variant family has ^{54}Ca , ^{78}Ni and ^{138}Sn in the fitted data set where asymmetry $\delta \sim 0.26 - 0.28$. The χ_0^2 function is still rather flat, making it tenuous to give a reasonable bound on the value of Δr_{np} of ^{208}Pb . The role of ultra neutron-rich nuclei in the SINPA-Variant family where nuclei with $\delta > 0.3$ (e.g. ^{24}O , ^{30}Ne , ^{36}Mg , ^{58}Ca) are further included in the fitting protocol are eminently evident in Fig 1. As Δr_{np} of ^{208}Pb is correlated to L_0 [1, 40], one finds a tighter constraint on L_0 as well from SINPA as compared to SINPB (see Tab. III).

The two Variant families so constructed from selective optimization of the parameter set \mathbf{p}_0 keeping Δr_{np} of ^{208}Pb fixed should affect the calculated binding energies. In Fig. 2 binding energy differences of three isotopic chains of O, Ca and Ni extracted from models SINPB and SINPA ($\Delta r_{np}(^{208}\text{Pb}) = 0.241$ fm and 0.183 fm, respectively at absolute minima of χ_0^2 , see Fig. 1) are plotted as a function of asymmetry δ . The differences in the

binding energies so calculated for all the isotopic chains show significant enhancement when one goes from δ just below 0.3 to higher values [23]. Nuclei beyond $\delta = 0.3$ thus show a high sensitivity towards Δr_{np} of ^{208}Pb . Several experimental efforts are being made to accurately measure binding energies of these exotic nuclei. These measurements may impose very tight constraint on the value of Δr_{np} of ^{208}Pb .

The sensitivity of a given parameter to a particular data can be determined in terms of the sensitivity matrix of dimension $N_p \times N_d$ defined as [41, 42],

$$S(\mathbf{p}) = [\hat{J}(\mathbf{p})\hat{J}^T(\mathbf{p})]^{-1}\hat{J}(\mathbf{p}). \quad (12)$$

Here $\hat{J}(\mathbf{p})$ is the Jacobian matrix with the same dimension as $S(\mathbf{p})$; its elements are given as,

$$\hat{J}_{\alpha i} = \frac{1}{\Delta\mathcal{O}_i} \left(\frac{\partial\mathcal{O}_i}{\partial p_\alpha} \right)_{\mathbf{p}_0}. \quad (13)$$

The sensitivity of the parameter p_α to the i -th data is given by $S_{\alpha i}^2$ which is normalized to $\sum_{i=1}^{N_d} S_{\alpha i}^2 = 1$. The relative sensitivity for a subset of data can likewise be obtained by summing $S_{\alpha i}^2$ over that subset.

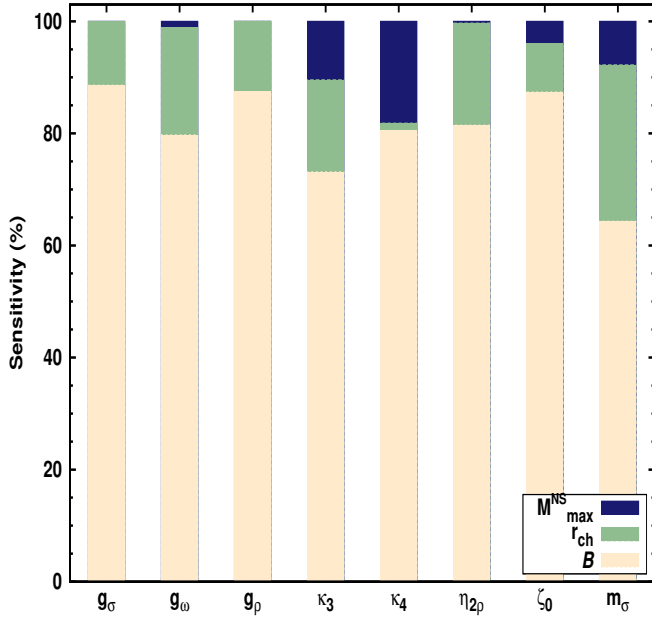


FIG. 3: (Color online) Relative sensitivity of different parameters of the effective Lagrangian density to three groups of fit data used in optimization of SINPA. These groups are nuclear binding energies (B), charge radii (r_{ch}) and maximum mass of neutron star (M_{max}^{NS}).

We employed the sensitivity analysis in model SINPA to understand the impact of the new fit-data considered to optimize it. In Fig. 3 the relative sensitivity of different parameters of the effective Lagrangian density to three broad data-types (binding energies B , charge radii r_{ch} of finite nuclei and maximum mass of neutron star

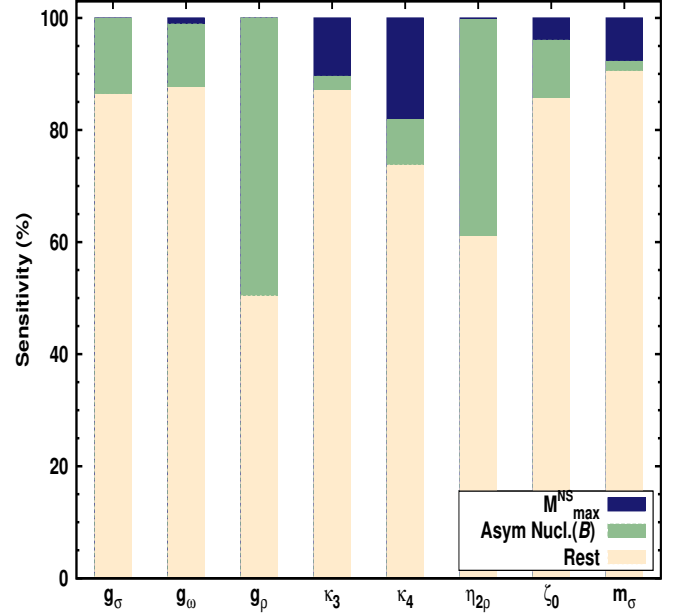


FIG. 4: (Color online) Same as Fig. 3, but, with different grouping of the fit data of finite nuclei. One group contains binding energies of highly asymmetric nuclei (^{24}O , ^{30}Ne , ^{36}Mg and ^{58}Ca) and another contains remaining fit data on the finite nuclei.

M_{max}^{NS}) are displayed. It is evident that all the parameters are maximally sensitive ($>65\%$) to the binding energies of nuclei. The higher relative sensitivity of the parameters to the binding energies of nuclei can be attributed partly to their large number used in the fit. The parameter κ_4 shows almost no sensitivity towards the charge radii. The parameters κ_3 , κ_4 and m_σ are seen to be appreciably sensitive to the single data of neutron star M_{max}^{NS} as they have a crucial role in the determination of the high density behavior of the nuclear EoS which in turn governs the value of M_{max}^{NS} .

In Fig. 4 we perform the analysis by regrouping the data on binding energies and charge radii so that the sensitivity of the RMF model parameters to the binding energies of highly asymmetric nuclei can be assessed. One of the group consists of only the binding energies of ^{24}O , ^{30}Ne , ^{36}Mg and ^{58}Ca nuclei, while the other group contains the remaining data on the finite nuclei. One can not fail to notice that, the parameters g_ρ and $\eta_{2\rho}$, which control the isovector part of the effective Lagrangian, are relatively more sensitive ($\sim 40\%$) to the binding energies of highly asymmetric nuclei. The sensitivity of g_ρ and $\eta_{2\rho}$ to the value of M_{max}^{NS} is not observed in Figs. 3 and 4 partly because M_{max}^{NS} is a single datum, but mainly because it is overshadowed by the relative contributions to the sensitivity from the binding energies of asymmetric nuclei.

In Fig. 5 we display at saturation density ρ_0 the sensitivity of different empirical data pertaining to the nuclear matter to the data-set used in the optimization of

the model SINPA. To do so, we used the same grouping of data as in Fig. 4. Since the parameters g_σ , g_ω etc. of the effective Lagrangian are optimally determined from the full data set, it is no wonder that the empirical nuclear matter data obtained from the energy density functional are maximally sensitive to the group of fit data "Rest", as it contains the largest number of data elements. The high sensitivity of C_{sym}^0 ($\sim 30\%$) and L_0 ($\sim 40\%$) to the binding energies of the highly asymmetric ^{24}O , ^{30}Ne , ^{36}Mg and ^{58}Ca nuclei, which form a very small subset of the data-set used in the optimization of SINPA (4 out of 30) is a reflection of the high sensitivity of the model parameters g_ρ and $\eta_{2\rho}$ to the masses of these highly asymmetric nuclei as seen earlier in Fig. 4. Appreciable sensitivity of all the nuclear matter properties to the single data on neutron star M_{max}^{NS} can not also be missed either. Accurate knowledge of M_{max}^{NS} is required for the precision determination of the EDF involving high densities beyond saturation, any small change in it thus may result in large change in the value of the nuclear matter properties (\mathcal{E}_0 , K_0 , ρ_0 , M_0^*) calculated from the EDF. This can be appreciated from the sensitivity of κ_3 , κ_4 and partly ζ_0 (governing the scalar mass and the number density) on M_{max}^{NS} displayed in Fig. 4. The not-too-insignificant sensitivity of C_{sym}^0 and L_0 to M_{max}^{NS} demands attention. It stems from the dependence of the kinetic part of $C_{sym}(\rho)$ on M^* (Eq. (7)) whose value at saturation density is found appreciably sensitive to the maximum mass of neutron star. The value of σ -field determining the effective mass of nucleon depends on the coupling constants g_σ , κ_3 , κ_4 and the value of m_σ . High sensitivity of these coupling constants to M_{max}^{NS} (see Figs. 3 and 4) gets reflected in the sensitivity analysis of the symmetry energy parameters to M_{max}^{NS} .

To this end, we would like to mention that, the binding energies for finite nuclei near neutron drip line as considered in the present work may be in general sensitive to the way pairing correlations are treated. We compare our results with those obtained in Ref. [23] calculated for neutron-rich nuclei for the same form of Lagrangian density but with 'exact' treatment of pairing. We find that the sensitivity of binding energies of neutron-rich isotopes of Oxygen and Calcium nuclei to the Δr_{np} of ^{208}Pb is very similar. To be specific, in Ref. [23], the binding energy of ^{24}O increases by ~ 4 MeV when the neutron-skin thickness (Δr_{np}) of ^{208}Pb changes from 0.16 fm to 0.28 fm. Similar trend is observed in our present calculation. For ^{24}O , the gain in binding energy is ~ 2 MeV when Δr_{np} changes from 0.18 fm (SINPA) to 0.24 fm (SINPB). The same feature is seen for the case of ^{58}Ca . However, for more precise determination of neutron-skin thickness in heavy nuclei on the basis of nuclear masses, Relativistic Hartree Bogoliubov (RHB) calculation for pairing for nuclei near the drip line is preferable [43–45]; this was not pursued in the present calculation.

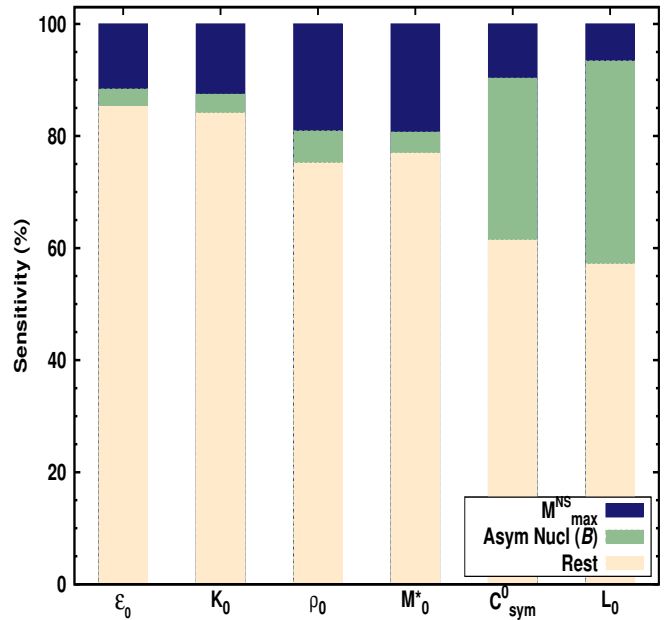


FIG. 5: (Color online) Relative sensitivity of the nuclear matter properties at saturation density to the fit data of SINPA with the same grouping as in Fig. 4.

D. Nuclear Matter properties at high density

We extended our calculation of nuclear matter properties with both the models SINPB and SINPA at densities beyond saturation. This provides valuable informations to construct theories for dense nuclear systems viz. neutron star and several other astrophysical objects from EoS so constrained at saturation density. In Fig. 6 we have plotted different nuclear matter properties, e.g. binding energy per nucleon for symmetric matter \mathcal{E} (Fig. 6(a)), symmetry energy coefficient C_{sym} (Fig 6(b)) and its density derivative L (Fig. 6(c)) as a function of density ρ/ρ_0 for the models SINPB (turquoise) and SINPA (black-pattern) along with their associated errors. The errors are calculated within the covariance analysis. The energy per nucleon \mathcal{E} in the explored density region for SINPB and SINPA are almost identical as seen from Fig. 6(a). Most stringent constraint on the values of \mathcal{E} appear at $\rho \sim \rho_0$ for both the models and they grow as one moves away from ρ_0 [46]. In Fig. 6(b) allowed regions of C_{sym} show similar trend for SINPB and SINPA, both of them having their minimum variance at $\rho \sim 0.7\rho_0$ [47]. However, a significant improvement is observed over the errors on C_{sym} for SINPA in comparison to SINPB at higher densities. Comparison of calculated electric dipole polarizability of ^{208}Pb from several Skyrme and RMF interactions with the corresponding experimental data recently yielded a very tightly constrained value of C_{sym} at density $\rho_0/3$, $C_{sym}(\rho_0/3) = 15.91 \pm 0.99$ MeV [48]. It is interesting to note that the model SINPB has overlap with this constraint at the lower end, $C_{sym}(\rho_0/3) = 13.69$

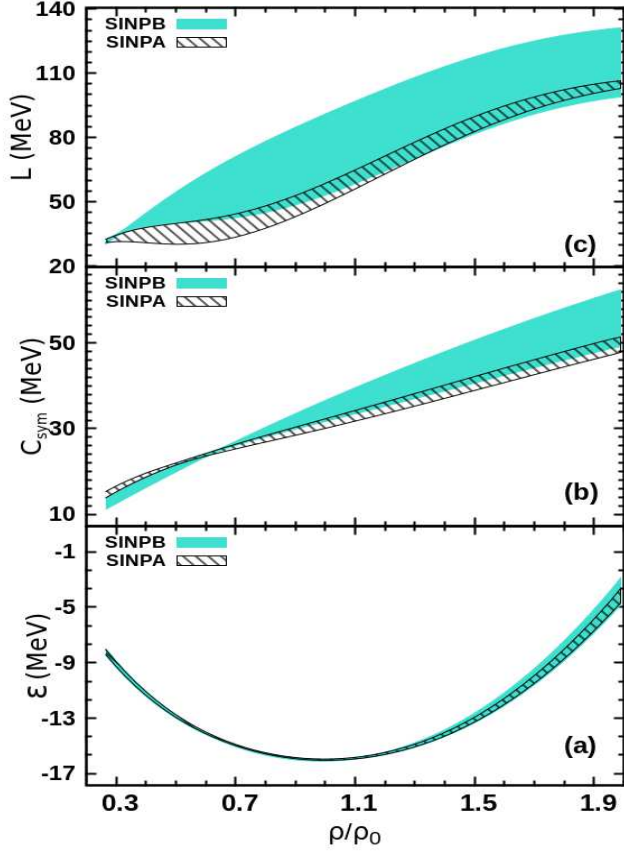


FIG. 6: (Color online) Binding energy per nucleon for symmetric matter \mathcal{E} , symmetry energy parameter C_{sym} and its density derivative L along with their errors as a function of density ρ/ρ_0 for SINPB and SINPA.

- 16.31 MeV, whereas SINPA agrees with this result at the higher end, $C_{sym}(\rho_0/3) = 16.41 - 17.67$ MeV.

In Fig. 6(c) a curious behavior in the variance of L with density was observed. For the model SINPB, the variance in L grows up to a certain density $\sim \rho_0$ and from there onwards it remained almost constant all the way up to $2\rho_0$. In contrast, in SINPA error on L grows only up to $\rho \sim 0.7\rho_0$ and shows a monotonically decreasing trend afterwards. This particular result may appear intriguing. A model primarily obtained by fitting some ground state properties of finite nuclei, where concerned central density is $\sim \rho_0$ and average density is $\sim 0.7\rho_0$ is not normally expected to show better constraint on nuclear matter properties at ultra-saturation densities. To investigate this, we looked into the expression of C_{sym} as a function of density given in Eq. (7). C_{sym} has a dependence on m_ρ^{*2} , the square of the effective mass of ρ meson. The density variation of m_ρ^{*2} for both the models are displayed in Fig. 7. A rapid difference in the value of m_ρ^{*2} (scaled by 10^5) calculated in models SINPA and SINPB builds up with increasing density. As the value of the parameter $\eta_{2\rho}$ is much larger in SINPA (38.18) compared to that in SINPB (13.49) [see Table I], at high

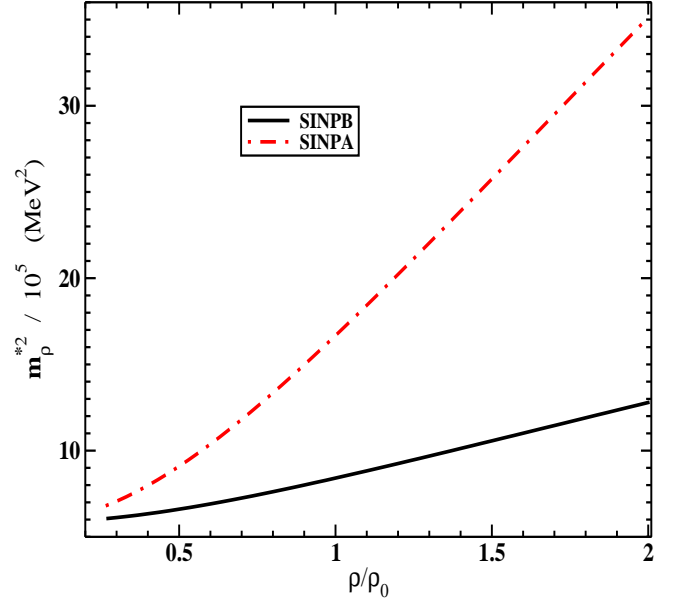


FIG. 7: (Color online) Square of the effective mass of ρ meson (scaled by 10^5) as a function of density ρ/ρ_0 plotted for SINPB and SINPA.

densities the second term in the expression of C_{sym} (Eq. (7)) gets diluted due to m_ρ^{*2} (Eq. (9)) by a much greater rate for the model SINPA in comparison to SINPB. This explains why the error on C_{sym} grows at much faster rate in SINPB than in SINPA. Now, if one takes density derivative of C_{sym} , the second term in Eq. (7) gives rise to two terms with $\eta_{2\rho}$ in the denominator for the expression of L as a function of density due to varying ω field value. That is why $\eta_{2\rho}$ becomes a very crucial factor for the values of L at higher densities. This fact explains why in SINPA error on L decreases at higher densities, whereas in SINPB it remains almost constant as shown in Fig. 6(c).

IV. SUMMARY AND CONCLUSIONS

To sum up, we have made an investigation in this paper on the extraction of the precision information from experimental data on the isovector content of the nuclear interaction and their observable derivatives like the symmetry energy of nuclear matter and its density slope L_0 at saturation density. The relativistic mean field model is chosen as the framework for the realization of this goal. A comparative study of the covariance analysis of the interaction strengths and the symmetry observables (C_{sym}^0 , L_0 , Δr_{np} of ^{208}Pb) made with two models SINPB (one that included in the fit data selective isovector sensitive information on observables from nearly symmetric and asymmetric nuclei) and SINPA (which included further data from extremely asymmetric nuclei right at the edge of neutron drip line with neutron to proton ratio ~ 2

and the observed maximum mass M_{max}^{NS} of neutron star) shows that the nuclear symmetry energy properties and the neutron skin Δr_{np} of ^{208}Pb are determined in much narrower constraints from the latter model. This is a pointer to the necessity of inclusion of extremely neutron-rich systems in any data analysis for filtering out information on isovector entities in the nuclear interaction. Noticeably growing difference in the binding energies of isotopes of some chosen nuclei with nuclear asymmetry

δ beyond ~ 0.3 , calculated in models SINPA and SINPB and also in a somewhat related paper [23] tend to confirm this. The conclusion is further reinforced from the sensitivity analysis of the different model parameters entering the nuclear effective interaction to the experimental data set taken for such an analysis. To check the robustness of such calculational outcome, it may be interesting to extend the investigation to other different versions of the mean-field models, both relativistic and non-relativistic.

-
- [1] M. Centelles, X. Roca-Maza, X. Viñas, and M. Warda, Phys. Rev. Lett. **102**, 122502 (2009).
 - [2] P. Möller, W. D. Myers, H. Sagawa, and S. Yoshida, Phys. Rev. Lett **108**, 052501 (2012).
 - [3] H. Jiang, G. J. Fu, Y. M. Zhao, and A. Arima, Phys. Rev. C **85**, 024301 (2012).
 - [4] B. K. Agrawal, J. N. De, and S. K. Samaddar, Phys. Rev. Lett. **109**, 262501 (2012).
 - [5] B. K. Agrawal, J. N. De, S. K. Samaddar, G. Colò, and A. Sulaksono, Phys. Rev. C **87**, 051306(R) (2013).
 - [6] J. Liu, Z. Ren, C. Xu, and R. Xu, Phys. Rev. C **88**, 024324 (2013).
 - [7] P. Danielewicz and J. Lee, Nuclear Physics A **818**, 36 (2009), ISSN 0375-9474.
 - [8] M. Liu, N. Wang, Z. Li, and F. Zhang, Phys. Rev. C **82**, 064306 (2010).
 - [9] N. Wang, L. Ou, and M. Liu, Phys. Rev. C **87**, 034327 (2013).
 - [10] D. V. Shetty, S. J. Yennello, and G. A. Souliotis, Phys. Rev. C **75**, 034602 (2007).
 - [11] M. A. Famiano and *et. al*, Phys. Rev. Lett. **97**, 052701 (2006).
 - [12] B.-A. Li, L.-W. Chen, and C. M. Ko, Phys. Rep. **464**, 113 (2008).
 - [13] X. Roca-Maza, M. Brenna, B. K. Agrawal, P. F. Bortignon, G. Colò, L.-G. Cao, N. Paar, and D. Vretenar, Phys. Rev. C **87**, 034301 (2013).
 - [14] X. Roca-Maza, M. Brenna, G. Colò, M. Centelles, X. Viñas, B. K. Agrawal, N. Paar, D. Vretenar, and J. Piekarewicz, Phys. Rev. C **88**, 024316 (2013).
 - [15] A. W. Steiner and S. Gandolfi, Phys. Rev. Lett. **108**, 081102 (2012).
 - [16] M. Dutra, O. Lourenco, J. S. SáMartins, A. Delfino, J. R. Stone, and P. D. Stevenson, Phys. Rev. C **85**, 035201 (2012).
 - [17] M. Dutra, O. Lourenço, S. S. Avancini, B. V. Carlson, A. Delfino, D. P. Menezes, C. Providência, S. Typel, and J. R. Stone, Phys. Rev. C **90**, 055203 (2014).
 - [18] T. Nikšić, D. Vretenar, and P. Ring, Phys. Rev. C **78**, 034318 (2008).
 - [19] P. W. Zhao, Z. P. Li, J. M. Yao, and J. Meng, Phys. Rev. C **82**, 054319 (2010).
 - [20] J. Dong, W. Zuo, J. Gu, and U. Lombardo, Phys. Rev. C **85**, 034308 (2012).
 - [21] B. A. Brown, W. A. Richter, and R. Lindsay, Phys. Lett. B **483**, 49 (2000).
 - [22] C. Mondal, B. K. Agrawal, and J. N. De, Phys. Rev. C **92**, 024302 (2015).
 - [23] W.-C. Chen and J. Piekarewicz, Physics Letters B **748**, 284 (2015).
 - [24] B. G. Todd-Rutel and J. Piekarewicz, Phys. Rev. Lett **95**, 122501 (2005).
 - [25] R. Furnstahl, B. D. Serot, and H.-B. Tang, Nucl. Phys. **A615**, 441 (1997).
 - [26] J. Boguta and A. R. Bodmer, Nucl. Phys. **A292**, 413 (1977).
 - [27] J. Boguta and H. Stoecker, Phys.Lett. **B120**, 289 (1983).
 - [28] R. Furnstahl, Nucl. Phys. **A706**, 85 (2002).
 - [29] T. Sil, M. Centelles, X. Viñas., and J. Piekarewicz, Phys. Rev. **C71**, 045502 (2005).
 - [30] P. R. Bevington, Data Reduction and Error Analysis for the Physical Sciences (McGraw-Hill, New York, 1969).
 - [31] M. Wang, G. Audi, A. Wapstra, F. Kondev, M. MacCormick, X. Xu, and B. Pfeiffer, Chinese Physics C **36**, 1603 (2012).
 - [32] A. T. Gallant, J. C. Bale, T. Brunner, U. Chowdhury, S. Ettenauer, A. Lennarz, D. Robertson, V. V. Simon, A. Chaudhuri, J. D. Holt, et al., Phys. Rev. Lett. **109**, 032506 (2012).
 - [33] F. Wienholtz and *et. al.*, Nature **498**, 346 (2013).
 - [34] I. Angeli and K. Marinova, Atomic Data and Nuclear Data Tables **99**, 69 (2013).
 - [35] P. B. Demorest, T. Pennucci, S. M. Ransom, M. S. E. Roberts, and J. W. T. Hessels, Nature **467**, 1081 (2010).
 - [36] J. Antoniadis and *et. al*, Science **340**, 448 (2013).
 - [37] P. Klüpfel, P.-G. Reinhard, T. J. Bürvenich, and J. A. Maruhn, Phys. Rev. C **79**, 034310 (2009).
 - [38] C. J. Horowitz and J. Piekarewicz, Phys. Rev. C **64**, 062802(R) (2001).
 - [39] R. Wang and L.-W. Chen, Phys. Rev. C **92**, 031303 (2015).
 - [40] L.-W. Chen, C. M. Ko, and B.-A. Li, Phys. Rev. C **72**, 064309 (2005).
 - [41] M. Kortelainen, T. Lesinski, J. Moré, W. Nazarewicz, J. Sarich, N. Schunck, M. V. Stoitsov, and S. Wild, Phys. Rev. C **82**, 024313 (2010).
 - [42] J. Dobaczewski, W. Nazarewicz, and P.-G. Reinhard, J Phys. G **41**, 074001 (2014).
 - [43] D. Vretenar, T. Nikšić, and P. Ring, Phys. Rev. C **68**, 024310 (2003).
 - [44] T. Nikšić, N. Paar, D. Vretenar, and P. Ring, Computer Physics Communications **185**, 1808 (2014).
 - [45] G. A. Lalazissis, D. Vretenar, P. Ring, M. Stoitsov, and L. M. Robledo, Phys. Rev. C **60**, 014310 (1999).
 - [46] J. N. De, S. K. Samaddar, and B. K. Agrawal, Phys. Rev. C **92**, 014304 (2015).
 - [47] Z. Zhang and L.-W. Chen, Physics Letters B **726**, 234 (2013).
 - [48] Z. Zhang and L.-W. Chen, Phys. Rev. C **92**, 031301 (2015).